



HAL
open science

”Solid conduction effects and design criteria in moving bed heat exchangers”

J.A. Almendros-Ibáñez, A. Soria-Verdugo, U. Ruiz-Rivas, D. Santana

► To cite this version:

J.A. Almendros-Ibáñez, A. Soria-Verdugo, U. Ruiz-Rivas, D. Santana. ”Solid conduction effects and design criteria in moving bed heat exchangers”. Applied Thermal Engineering, 2011, 31 (6-7), pp.1200. 10.1016/j.applthermaleng.2010.12.021 . hal-00723970

HAL Id: hal-00723970

<https://hal.science/hal-00723970>

Submitted on 16 Aug 2012

HAL is a multi-disciplinary open access archive for the deposit and dissemination of scientific research documents, whether they are published or not. The documents may come from teaching and research institutions in France or abroad, or from public or private research centers.

L’archive ouverte pluridisciplinaire **HAL**, est destinée au dépôt et à la diffusion de documents scientifiques de niveau recherche, publiés ou non, émanant des établissements d’enseignement et de recherche français ou étrangers, des laboratoires publics ou privés.

Accepted Manuscript

Title: "Solid conduction effects and design criteria in moving bed heat exchangers"

Authors: J.A. Almendros-Ibáñez, A. Soria-Verdugo, U. Ruiz-Rivas, D. Santana

PII: S1359-4311(10)00537-5

DOI: [10.1016/j.applthermaleng.2010.12.021](https://doi.org/10.1016/j.applthermaleng.2010.12.021)

Reference: ATE 3345

To appear in: *Applied Thermal Engineering*

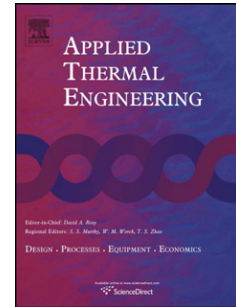
Received Date: 26 July 2010

Revised Date: 7 December 2010

Accepted Date: 12 December 2010

Please cite this article as: J.A. Almendros-Ibáñez, A. Soria-Verdugo, U. Ruiz-Rivas, D. Santana. "Solid conduction effects and design criteria in moving bed heat exchangers", *Applied Thermal Engineering* (2010), doi: [10.1016/j.applthermaleng.2010.12.021](https://doi.org/10.1016/j.applthermaleng.2010.12.021)

This is a PDF file of an unedited manuscript that has been accepted for publication. As a service to our customers we are providing this early version of the manuscript. The manuscript will undergo copyediting, typesetting, and review of the resulting proof before it is published in its final form. Please note that during the production process errors may be discovered which could affect the content, and all legal disclaimers that apply to the journal pertain.



Solid conduction effects and design criteria in moving bed heat exchangers

J.A. Almendros-Ibáñez^{a,b,*}, A. Soria-Verdugo^c, U. Ruiz-Rivas^c, D. Santana^c

^a*Escuela de Ingenieros Industriales, Dpto. de Mecánica Aplicada e Ingeniería de Proyectos, Castilla La Mancha University, Campus Universitario, 02071, Albacete, Spain*

^b*Renewable Energy Research Institute, Section of Solar and Energy Efficiency, Avda. de la Investigación s/n, 02071, Albacete, Spain*

^c*Carlos III University of Madrid, ISE Research Group, Thermal and Fluid Engineering Department, Avda. de la Universidad 30, 28911 Leganés, Madrid, Spain*

Abstract

This work presents a theoretical study of the energetic performance of a Moving Bed Heat Exchanger (MBHE), which consists on a flow of solid particles moving down that recovers heat from a gas flow percolating the solids in cross flow. In order to define the solid conduction effects, two solutions for the MBHE energy equations have been studied: an analytical solution considering only convection heat transfer (and neglecting solid conduction) and a numerical solution with the solid conductivity retained in the equations. In a second part, the power requirements of a MBHE (to pump the gas and to raise the down-flowing particles) are confronted with the heat transferred considering the variation of design parameters, such as gas and solids velocities, solids particle diameter or MBHE dimensions.

The numerical results show that solid conductivity reduces the global efficiency of the heat exchanger. Therefore, a selection criterium for the solids can be established, in which their thermal conductivity should be minimized to avoid conduction through the solid phase, but to a limit in order to ensure that temperature differences inside an individual solid particle remain small. Regarding the other energy interactions involved in the system, these are at least one order of magnitude lower than the heat exchanged. Nevertheless, for a proper analysis of the system the efficiency of the devices used to pump the gas and to raise the particles and the relative costs of the different energy

*Corresponding author: e-mail: jose.almendros@uclm.es, T: +34967599200

forms present in the system should be taken into account.

Keywords: Moving Bed Heat Exchanger, Heat transfer, Biot number, Packed bed

1. Introduction

Moving Bed Heat Exchangers (MBHE hereafter, and often called packed beds heat exchangers) are widely used in industry, for applications involving heat recovery, solids drying, filtering or thermochemical conversion processes. Compared with other systems, they provide a large heat transfer area in a reduced volume and, concerning filtering, they avoid common operational problems that are typical of fixed-bed or ceramic filters, such as the pressure drop increase during operation.

Several studies can be found in the literature concerning flow patterns and particles velocity in moving beds, as for example the works by Hsiau et al. [1–3] as well as on the heat transfer between gas and particles in fixed or moving beds [4–9]. Moving beds are often found in heat recovery systems, like the usual counter-flow regenerator that transfers heat between two fluid flows. Also, they can be used to recover heat from a flow of solids to another flow of solids [10] or to dry a flow of solids [11]. On the other hand, different equipments have been proposed for hot gas particulate removal, such as electrostatic precipitators, ceramic filters, scrubbers, bag filters and granular filters [1, 4, 12, 13]. Smid et al. [14] made a complete review of the patent literature about moving bed filters and their equipment in different countries around the world. MBHE are increasing in interest as a key component in integrated gasification combined cycles, as well as in pressurized fluidized bed combustors, due to two main advantages: their capacity to properly filter the gas stream at high temperatures and their suitability to be used also as heat exchangers. More recently, MBHE has also been employed in novel thermochemical conversion processes for the production of uranium tetrafluoride [15] or for catalytic naphtha reforming [16].

The bed material used in the MBHE depends on the application. For high temperature heat exchange and filtration, alumina and silica sand (with a size ranging between 0.5 and 2.0 mm) are typically used in industrial applications [13, 17]. Spheres of steel are also widely used [6, 9]. Recently, Macias-Machin et al. [18] presented “lapilly”, a new material for gas filtration applications. In applications different to heat recovery and gas filtration specific materials can

33 be used. For example, Niksiar and Rahimi [15] reduced granulated uranium
 34 trioxide in a moving bed during the process to obtain uranium tetrafluoride.

35 This article focuses on the design of a MBHE based on energy criteria
 36 (increasing heat transfer without dramatically increasing the power consump-
 37 tion needed to move the two flows) with emphasis on solid conduction effects.
 38 On a previous article [19] we presented an exergy analysis of the MBHE, in
 39 which an optimized length (in the fluid flow direction) and solids particle
 40 diameter were obtained. In the following, the relative importance of conduc-
 41 tion in the solid phase is analysed and different approaches are presented to
 42 define the adequate parameters (particle diameter and the velocities of both
 43 flows) for a given application.

44 In the results showed along this article, the fluid is air and there is no
 45 mass transfer between fluid and solids (i.e. no solids drying, filtering or phase
 46 change). The nominal values of the data are obtained from the experimental
 47 set-up of Henriquez and Macías-Machín [9], which are summarized in Ta-
 48 ble 1. The properties of the solids showed in this table correspond with the
 49 properties of the spheres of steel used by Henriquez and Macías-Machín [9].

50 Figure 1(a) shows a general scheme of the MBHE geometry. The solids
 51 move down in the positive y direction and the gas percolates through the solid
 52 particles in crossflow (moving from left to right), in the positive x direction.
 53 In the following we will assume the 2D geometry showed in Figure 1(b) for
 54 the heat transfer analysis.

55 [Table 1 about here.]

56 [Figure 1 about here.]

57 2. Governing equations

58 The general two-phase equations governing heat transfer for the MBHE
 59 showed in Figure 1(a) are given by the equation system (1)-(2). Heat losses
 60 to the surroundings, radiation heat transfer and the loss of solids potential
 61 energy are neglected in this analysis.

$$\varepsilon \rho_g c_{p,g} \left(\frac{\partial T}{\partial t} + \mathbf{u}_g \cdot \nabla T \right) = \nabla \cdot (k_g \nabla T) + h_s a_s (\theta - T) \quad (1)$$

$$(1 - \varepsilon) \rho_s c_s \left(\frac{\partial \theta}{\partial t} + \mathbf{u}_s \cdot \nabla \theta \right) = \nabla \cdot (k_s \nabla \theta) + h_s a_s (T - \theta) \quad (2)$$

62 T and θ are the gas and solid temperature respectively and a_s is the superficial
63 particle area per unit of volume. When the fluid used in the MBHE is a gas
64 the diffusion term of equation (1) is usually orders of magnitude lower than
65 the convective term and can be neglected in the calculations. In contrast the
66 solid conductivity, specially for metallic materials, can not be neglected and
67 it is retained in the calculations.

68 A common simplification in MBHE modeling is the assumption of plug
69 flow in both phases (gas and solids), which is equivalent to assuming a con-
70 stant voidage in the bed and uniform velocity profiles for both phases. This
71 is not true close to the walls of the bed, so a much more complex modeling
72 is needed for narrow beds. A number of works has studied the particles and
73 gas flow close to the walls, both numerically and experimentally, in order to
74 state its characteristics and relevance. The MiDi research group [20] ana-
75 lyzed the behavior of dense assemblies of dry grains submitted to continuous
76 shear deformation. For vertical chute-flows, where gravity drives the material
77 down between the walls, both particle velocity profile and bed porosity pro-
78 file are characterized by a plug region in the central part of the channel and
79 shear zones near the walls, where particle velocity and porosity vary. The
80 thickness of such zones is of the order of 5 to 6 particle diameters for nearly
81 spherical particles. This is also in agreement with the work of Nedderman
82 and Laohakul [21]. They also showed that the particle velocity at the walls is
83 25% below the velocity in the plug flow region for fully rough walls. Zou and
84 Yu [22] showed, for both loose and dense packing, that at a distance of 2.5
85 particle diameters from the wall, the mean wall porosity was approximately
86 10% above the bed core porosity. In contrast, Takahashi and Yanai [23] ob-
87 tained experimentally that only 2-3 column diameters are needed to reach
88 a stable plug-flow region. Moreover, they observed that, although the bed
89 porosity is slightly influenced by the velocity of the descending particles, this
90 influence vanishes when the solid-flow rate increases. Finally, their results
91 showed that particle velocity at wall is 0.7 to 0.8 the mean particle velocity at
92 bed core. Van Antwerpen et al. [24] have recently reviewed the correlations
93 to model the bed porosity and the effective thermal conductivity in packed
94 beds, showing that the local porosity behavior near the wall is similar to a
95 damped harmonic oscillator, whereas the porosity, averaged by a particle di-
96 ameter, can be approximated by an exponential function. Previously, Giese
97 et al. [25] proved, for different particle sizes, that the local gas velocity near
98 the wall has the same damped harmonic behavior as the local bed porosity.
99 But once again the local gas velocity oscillation damped when the Reynolds

100 particle number increases.

101 On the other hand, several works have dealt with the gas distribution
 102 in a moving bed and the plug flow assumption for the gas phase. Vort-
 103 meyer and Winter [26] reviewed experimental findings on the homogeneous
 104 behavior of packed beds and concluded that the limit of homogeneity lies
 105 much lower than predicted by a purely mathematical reasoning. They sug-
 106 gested that the limiting bed/particle diameter ratio must be at least 4 to
 107 consider gas plug flow in the packed bed. They concluded that, for their
 108 experimental conditions (ratios between the reactor diameter and the par-
 109 ticle size between 2 and 3), it was not necessary to extend the modelling
 110 by adding a variation in the radial or axial dispersion coefficient in the gas
 111 phase. On the other hand, Teplitskii et al. [27] showed that the thickness
 112 ratio between the filtration boundary layer and the viscous boundary layer
 113 is 1.78, the same ratio was found for the thickness of the filtration thermal
 114 boundary layer and the thermal sublayer. Therefore, the ratio of the filtra-
 115 tion boundary layer respect to particle diameter being equal to $0.33 Re_p^{-0.31}$
 116 for $Re_p > 120$ the thickness of both boundary layers are lower than a particle
 117 diameter. Also, and for Prandtl number of order unity, the thickness of the
 118 filtration thermal boundary layer and the thermal sublayer are of the same
 119 order of the particle diameter. Another source of gas maldistribution can be
 120 attributed to the cavity and pinning phenomena [28]. For a cross-flow, the
 121 particles close to the upstream face may leave the face and a cavity forms
 122 between the upstream face and the granular bed, while in the downstream
 123 face, the frictional force can be enough to stop the particles, forming a dead
 124 zone (pinning). Nevertheless, these two phenomena are only relevant for
 125 extremely high gas velocities.

126 In view of these findings [20–28], the assumption of plug flow for both
 127 solid and gas phase will be considered acceptable if the dimensions of the
 128 bed are larger than ten times the particle diameter. Therefore, assuming a
 129 2D geometry (see Figure 1(b)) and steady state conditions, the governing
 130 equations (1) and (2) can be written in compact and non-dimensional form
 131 as

$$\frac{\partial \hat{\theta}}{\partial \eta} - K_\xi \frac{\partial^2 \hat{\theta}}{\partial \xi^2} - K_\eta \frac{\partial^2 \hat{\theta}}{\partial \eta^2} = \hat{T} - \hat{\theta} = -\frac{\partial \hat{T}}{\partial \xi}, \quad (3)$$

132 where

$$\hat{\theta} = \frac{\theta - \theta_{in}}{T_{in} - \theta_{in}}, \quad \hat{T} = \frac{T - \theta_{in}}{T_{in} - \theta_{in}} \quad (4)$$

133 are the non-dimensional temperatures, varying between 0 and 1,

$$\xi = \frac{x h_s a_s}{\varepsilon \rho_g u_g c_{p,g}}, \quad \eta = \frac{y h_s a_s}{(1 - \varepsilon) \rho_s u_s c_s} \quad (5)$$

134 are the non-dimensional horizontal (x -direction) and vertical (y -direction)
135 coordinates respectively, and

$$K_\xi = \frac{h_s a_s k_{s,x}}{(\varepsilon \rho_g u_g c_{p,g})^2}, \quad K_\eta = \frac{h_s a_s k_{s,y}}{((1 - \varepsilon) \rho_s u_s c_s)^2} \quad (6)$$

136 are the non-dimensional conductivities in the direction of the gas flow and
137 in the direction of the solid flow respectively. The value of the thermal
138 conductivity in the direction of the gas flow was obtained using the correlation
139 proposed by Krupiczka [29], and the thermal conductivity in the direction of
140 the particle flow using the equation presented by Yagi et al. [6], as suggested
141 by Marb and Vortmeyer [30]. The convection heat transfer coefficient was
142 obtained with a correlation proposed by Achenbach [8].

143 In order to solve the non-dimensional equation system (3) a set of bound-
144 ary conditions is needed. The ones shown in Table 2 are considered to prop-
145 erly state the underlying physics, as shown by Marb and Vortmeyer [30].
146 The differential equation system (3) can be solved numerically using a finite
147 difference technique. The elliptic character of the equations is transformed
148 into parabolic adding a temporal derivative into the solid equation. The first
149 derivatives are discretized using an up-wind scheme and the second deriva-
150 tives using central differences. A more detailed description of the numerical
151 scheme can be seen in [19].

152 [Table 2 about here.]

153 The equation system (3) has also an analytical solution when the con-
154 duction terms are negligible, which is usually accepted for high Reynolds
155 numbers [31]. Then, the equation system (3) becomes:

$$\frac{\partial \hat{\theta}}{\partial \eta} = \hat{T} - \hat{\theta} = -\frac{\partial \hat{T}}{\partial \xi}. \quad (7)$$

156 The two boundary conditions needed to solve the equation system (7) are

$$\hat{T}_{\xi=0} = 1 \quad \text{and} \quad \hat{\theta}_{\eta=0} = 0. \quad (8)$$

157 With such conditions, according to Saastamoinen [32] and previous authors,
 158 the analytical solution for the non-dimensional gas and solid temperatures
 159 are

$$\hat{T} = e^{-\xi-\eta} \sum_{j=0}^{\infty} \frac{\eta^j}{j!} \sum_{k=0}^j \frac{\xi^k}{k!} \quad (9)$$

$$\hat{\theta} = 1 - e^{-\eta-\xi} \sum_{j=0}^{\infty} \frac{\xi^j}{j!} \sum_{k=0}^j \frac{\eta^k}{k!} \quad (10)$$

160 3. Analysis

161 3.1. Heat transfer and conduction effects

162 First we will discuss the heat transfer issues and the relative importance
 163 of conduction effects. As shown in Soria-Verdugo et al. [19] in a study that
 164 neglected solid conduction effects, the heat transfer process is optimized for
 165 both flows when

$$\xi_{x=L} = \eta_{y=H}. \quad (11)$$

166 If one of the non-dimensional parameters of this equation is larger than the
 167 other, a certain part of the flow coming perpendicular to the larger length
 168 will exit the MBHE barely undisturbed (with a temperature near to its inlet
 169 temperature). Therefore, Equation (11) should be fulfilled for a proper heat
 170 exchange (or it may not when other issues are of paramount importance, such
 171 as a proper filtering). This will be denoted as a “square” MBHE throughout
 172 the article, being square only in this non-dimensional sense. Going back to
 173 Equations (5) and using typical velocities and properties for solids and air, it
 174 can be stated that this square condition usually means that the H dimension
 175 is three times larger than the L dimension, with possible variations ranging
 176 from almost equal values for both dimensions, to H ten times larger than
 177 L . Rearranging Equation (11), it also states that the product of the mass
 178 flow and the specific heat should be equal for both flows (fluid and solids), a
 179 typical result in heat exchangers.

$$\dot{m}_s c_s = \rho_s (1 - \varepsilon) L B u_s c_s = \rho_g \varepsilon H B u_g c_{p,g} = \dot{m}_g c_{p,g} \quad (12)$$

180 Moreover, Equation (12) defines the ratio between MBHE length and
 181 height as a function of solid and fluid velocities, and of general properties,
 182 giving variations as stated above. Note that the two non-dimensional lengths

183 of Equation (11) are not supposed to be limited by unity. With the previously
 184 mentioned MBHE of Henriquez and Macías-Machín [9], which represents a
 185 rather small MBHE, both non-dimensional lengths are around 350. Table 3
 186 shows the non-dimensional parameters obtained with the nominal data of
 187 Henriquez and Macias-Machín [9] summarised in Table 1.

188 [Table 3 about here.]

189 Figure 2(a) shows the non-dimensional gas temperature profiles, when
 190 solid conductivity is neglected, for a “square” heat exchanger of the same size
 191 of our nominal MBHE. In this situation, an analytical solution (Equation (9))
 192 can be used. Heat is only transferred by convection from the hot gas to the
 193 cold solids in a narrow region of the bed.

194 Now we will consider solid conduction effects. Figure 2(b) shows the
 195 non-dimensional gas temperature profiles for the nominal data showed in
 196 Table 1 diminishing the solid conductivity one order of magnitude (from
 197 $k_s = 15 \text{ W/(m K)}$ to $k_s = 1.5 \text{ W/(m K)}$), which results in non-dimensional
 198 conductivities of $K_\xi = 5.41$ and $K_\eta = 0.46$. Figure 2(c) shows the same
 199 curves for the nominal data ($k_s = 15 \text{ W/(m K)}$). In contrast to Figure 2(a),
 200 when conduction is taken into account, part of the heat is transferred by
 201 conduction through the solid phase. As a result, the width of the region where
 202 T and θ change increases. Higher conductivities K_ξ and K_η implies larger
 203 regions of temperature variation. Also, the different boundary conditions
 204 applied to both flows when conduction is considered changes the symmetry
 205 of the problem (although in a feeble way), as can be seen in the inlet and
 206 outlet of particles in Figure 2(c). Nevertheless, symmetry is still important
 207 and Equation (11) can be used as an adequate design criteria.

208 [Figure 2 about here.]

209 The variations between Figures 2(a), 2(b) and 2(c) can be largely at-
 210 tributed to the conduction term in the gas flow direction, K_ξ , which is roughly
 211 an order of magnitude larger than the conduction term in the perpendicular
 212 direction K_η . This is a consequence of H being larger than L , as stated above,
 213 because when the restriction of Equation (12) is used over the definitions of
 214 Equation (6), it follows that

$$\frac{K_\xi}{K_\eta} = \frac{k_{s,x}}{k_{s,y}} \left(\frac{H}{L} \right)^2 \sim \left(\frac{H}{L} \right)^2 \gg 1. \quad (13)$$

215 The main feature of solid conduction is that the net heat transfer between
 216 solids and fluid diminishes, as the initially hot flow (an air flow in this case)
 217 exits the MBHE with a higher mean outlet temperature in Figure 2(c) than
 218 in Figure 2(a), due to the larger heat exchange region. Figure 2(b) shows an
 219 intermediate case. This is a rather surprising result, as a higher capability to
 220 conduct heat results in a global heat transfer decrease. Therefore, avoiding
 221 conduction effects in the solids will maximize the heat transferred by the
 222 MBHE.

223 Figure 3(a) shows the non-dimensional mean outlet temperature of the
 224 gas flow \bar{T}_{out} as a function of the MBHE non-dimensional length, for a
 225 “square” MBHE that follows Equation (11), and for five different conductiv-
 226 ities, ranging between $k_s = 0$ (neglecting conduction) and $k_s = 15 W/(m K)$
 227 (our nominal case). This temperature is directly related with the efficiency
 228 of the MBHE, defined as $\epsilon_{MBHE} = \dot{Q}/\dot{Q}_{max}$, by Equation (14)

$$\bar{T}_{out} = 1 - \epsilon_{MBHE}. \quad (14)$$

229 Thus, a value of \bar{T}_{out} close to zero implies a higher efficiency of the MBHE.
 230 The differences between zero, small, medium and large conduction terms are
 231 evident. The smaller solid conductivity cases show a fairly similar response
 232 than that of the non conduction case for lengths larger than 100. But for the
 233 larger conduction case, the length should be larger than 350 to consider that
 234 the conduction effect has a feeble impact in the MBHE behaviour.

235 Therefore, for small values of the non-dimensional lengths $\xi_{x=L} = \eta_{y=H}$,
 236 conduction effects may prove important in diminishing the heat transferred
 237 in the MBHE. The effect can be minimized by reducing the conduction term
 238 (Equation (6)). As a consequence, if the influence of conduction heat trans-
 239 fer in the MBHE is more relevant, the size of the heat exchanger should
 240 increase to maintain its efficiency. Figure 3(b) shows the increase of the
 241 non-dimensional length of the MBHE for different solid conductivities with
 242 a heat exchanger efficiency of $\epsilon_{MBHE} = 90\%$ ($\bar{T}_{out} = 0.1$).

243 [Figure 3 about here.]

244 Once more, it might seem rather strange to diminish the solid conductiv-
 245 ity in a heat exchanger. Of course, a certain conductivity is needed in order
 246 to ascertain that the solids surface temperature and its inner temperature
 247 are similar, so that the convection heat transfer is not affected. Else, the
 248 heat transfer would be controlled by solid conduction inside the particles. In

249 order to avoid this effect, general theory [33] states that the Biot number
 250 should be

$$Bi = \frac{h_s d_p}{k_s} \leq 0.1. \quad (15)$$

251 Nevertheless, Equation (15) can be fulfilled for rather small values of the
 252 solid conductivity, considering small particles and small convection coeffi-
 253 cients based on the air-particle interaction.

254 Figure 4(a) shows a contour plot of the conduction term in the gas flow
 255 direction as a function of gas velocity and particle diameter for the steel
 256 spheres considered in the nominal case. Note that the convection coefficient
 257 depends on both gas velocity and particle size, increasing with the gas veloc-
 258 ity and decreasing when the particle size is increased. In view of this figure,
 259 in order to diminish the non-dimensional size of the MBHE (or to increase its
 260 efficiency with the same non-dimensional size), we could increase the particle
 261 size and/or the gas velocity, obtaining lower values of K_ξ .

262 Figure 4(b) shows a contour plot of the Biot number. In the range of
 263 particle sizes and gas velocity tested, the Biot number always fulfils Equa-
 264 tion (15). Thus, another parameter that can be modified to increase the ef-
 265 ficiency or decrease the size (if particle diameter and fluid velocity are fixed)
 266 is the conductivity of the solid media used in the MBHE (k_s). This mate-
 267 rial property affects both Biot number and non-dimensional conductivity K_ξ .
 268 Figure 4(c) shows the data of K_ξ , as a function of the gas velocity and the
 269 particle diameter, and for the minimum value of the solid conductivity that
 270 fulfils Equation (15). Figure 4(d) shows the contour plot of that minimum
 271 solid conductivity.

272 Therefore, increasing particle size and gas velocity and decreasing solid
 273 conductivity, the non-dimensional conductivity K_ξ is reduced. This fact re-
 274 sults in an improvement of the heat exchanger efficiency or in a reduction of
 275 its non-dimensional size. But note that a reduction of the non-dimensional
 276 size does not directly lead to a reduction of the actual size. This might be the
 277 case when varying d_p and u_g , as those two parameters are also involved in the
 278 definitions of the non-dimensional lengths (Equations (5)). Therefore, the ef-
 279 fect on the actual size is not straightforward and should be studied in each
 280 case. In contrast, the solid conductivity k_s only affects the non-dimensional
 281 conductivities but not any other parameter in the non-dimensional dimen-
 282 sions. Thus, a reduction of k_s implies directly a reduction of the actual
 283 MBHE size maintaining the rest of parameters constant.

284

[Figure 4 about here.]

285

286

287

288

289

290

291

292

293

294

295

296

297

298

299

300

For example, point A in Figures 4(a) and 4(b) represents the nominal MBHE of Henriquez and Macías-Machín [9]. If we increase the size of the particles from $d_p = 1 \text{ mm}$ to $d_p = 5 \text{ mm}$ with the same gas velocity, the non-dimensional solid conductivity K_ξ is reduced from $K_\xi = 51.12$ to $K_\xi \approx 4$ (point B in Figure 4(a)). Consequently, the Biot number increases from $Bi = 0.027$ to $Bi \approx 0.053$ (point B in Figure 4(b)), always fulfilling Equation (15). As commented previously, the efficiency of the MBHE can be further increased reducing the solid conductivity. According to the data summarized in Table 1, Henriquez and Macías-Machín [9] used particles with a solid conductivity of $k_s = 15 \text{ W}/(\text{m K})$. Reducing this solid conductivity to $k_s \approx 7.9 \text{ W}/(\text{m K})$ (see point C in Figure 4(d)) the non-dimensional conductivity K_ξ is reduced to a value of $K_\xi \approx 2.1$ (see point C in Figure 4(c)) in the limit of $Bi = 0.1$. Finally, introducing this data in Figure 3(b) we can check how the non-dimensional size needed to exchange 90% of the maximum heat is reduced to a value $\xi_{x=L} \approx 83$ (with the original data of Henriquez and Macías-Machín [9] a length of $\xi_{x=L} \approx 300$ is needed).

301

3.2. Heat transfer and power requirements

302

303

304

After this purely thermal analysis, one should take into account the other thermodynamic interactions, such as the power requirements to pump the fluid through the bed and to raise the solids.

305

306

307

308

For any MBHE, the heat transferred between gas and particles and the power consumed to pump the gas can be calculated per unit of gas mass flow with Equations (16) and (17), while the power required to raise the particles per unit of solids mass flow is expressed according Equation (18).

$$\frac{\dot{Q}}{\dot{m}_g} = c_{p,g} (\bar{T}_{in} - \bar{T}_{out}), \quad (16)$$

$$\frac{\dot{W}_g}{\dot{m}_g} = \frac{\Delta P}{\rho_g}, \quad (17)$$

$$\frac{\dot{W}_s}{\dot{m}_s} = g H. \quad (18)$$

309

The gas pressure drop ΔP can be obtained from Ergun equation [34]:

$$\Delta P = \rho_g \left(\frac{1 - \varepsilon}{\varepsilon^3} \right) \frac{L}{d_p} u_g^2 \left(\frac{150 (1 - \varepsilon) \mu_g}{d_p \rho_g u_g} + 1.75 \right). \quad (19)$$

310 Although Ergun equation was obtained for fixed (instead of moving) beds,
 311 the solids velocity in a MBHE is orders of magnitude lower than the gas
 312 velocity. Therefore, the particle movement can be neglected for pressure
 313 drop calculation in the majority of MBHE applications.

314 Equation (18) can be modified for a “square” MBHE taking into account
 315 Equation (12) as follows

$$\frac{\dot{W}_s}{\dot{m}_g} = g \frac{\rho_s}{\rho_g} \left(\frac{1 - \varepsilon}{\varepsilon} \right) L \frac{u_s}{u_g} \quad (20)$$

316 Equation (20) has been expressed per unit of gas mass flow (instead of solids
 317 flow) to be in concordance with Equations (16) and (17).

318 The results of the power requirements (Equations (17) and (20)) and
 319 heat transfer (Equation (16)) per unit of gas mass flow and for “square” heat
 320 exchanger are presented in Figure 5 as a function of the relevant parameters.
 321 The heat transfer is a function of the maximum temperature difference and of
 322 the non-dimensional length (that defines \bar{T}_{out} , as shown in figure 3(a)). The
 323 heat transferred is shown both assuming or neglecting conduction effects.
 324 The power consumed to pump the gas is a function of particle diameter and
 325 gas velocity, and the power consumed to raise the particles is a function
 326 of the gas and solids velocities. The rest of the parameters ($L = 0.15 m$,
 327 $\varepsilon = 0.4$) and properties (both densities, ρ_s and ρ_g , gas specific heat $c_{p,g}$ and
 328 the dynamic viscosity μ_g) are taken from the nominal case (see Table 1).

329 [Figure 5 about here.]

330 A quick glimpse at Figure 5 shows the relative importance of the different
 331 energy transfer mechanisms. The power to raise the particles is not relevant,
 332 even for high solid velocities. This is in accordance with our previous hy-
 333 pothesis of neglecting solid potential energy variations in Equations (1) and
 334 (2). The power needed to pump the gas is generally one to two orders of
 335 magnitude larger than the necessary power to raise the particles. The heat
 336 transfer is, of course, strongly dependant on the available temperature differ-
 337 ence between the two flows, but it is always one to two orders of magnitude
 338 larger than the power to pump the gas.

339 Nevertheless, the dependence of the energy variables with the MBHE di-
 340 mensions was not depicted in Figures 4 and 5. The required power to pump
 341 the gas and to raise the particles both increase linearly with the length of
 342 the bed L . In contrast, the heat transferred has a barely hyperbolic relation

343 with the non-dimensional length (in turn directly proportional to the actual
344 length). Therefore, for large non-dimensional lengths (see Figure 3(a)), in-
345 creasing the length of the MBHE will produce a linear increase of the power
346 requirements but with a feeble impact on the heat transferred.

347 Finally, it should be noted that, being the power values so different be-
348 tween heat transferred and mechanical power requirements, such a feeble
349 impact in heat may prove to add to a heat power increase larger than the
350 power required to further pump the gas. In such cases, the efficiency of blow-
351 ers and the higher cost of mechanical and/or electrical energy in relation to
352 heat should be taken into account. As a general trend, it seems wise to oper-
353 ate in the zone where the heat transfer reaches a certain stabilization to avoid
354 these larger costs and efficiency-based drawbacks. This stabilization point
355 can be established, taking into account the results of Figure 5 and Figure 3,
356 in the region where the heat exchanger efficiency reaches the 90%. There-
357 fore, an adequate non-dimensional length can be defined, as a function of the
358 conduction term incidence, as shown in Figure 3(b). Thus, a compromise be-
359 tween increasing heat transfer and increasing power requirements and MBHE
360 dimensions should be reached, which is not purely energetic and should con-
361 sider costs, pump and raiser efficiencies and the relative costs between heat
362 power and electric power.

363 4. Conclusions

364 The heat transfer analysis of the MBHE shows that large values of solid
365 conductivity in the solid phase reduces the efficiency of the heat exchanger
366 because the width of the region where heat is transferred is augmented, and
367 as a consequence the mean outlet temperature of the cold stream is reduced.
368 Consequently, solids with low conductivity should be selected, although a
369 minimum conductivity is necessary in order to assure that the temperature
370 is uniform in the solid phase, i.e. the Biot number should be lower than 0.1.
371 Thus, to increase the efficiency of a MBHE a compromise between particle
372 size and solid conductivity should be reached fulfilling the limit imposed by
373 the Biot number.

374 Regarding the other energy interactions (power consumed to pump the
375 gas and to raise the particles), these are orders of magnitude lower than the
376 heat transferred in the range of particle sizes and gas velocities studied and
377 for temperature differences larger than 100 K. Nevertheless, for a proper
378 analysis, the efficiency of the systems employed for pumping the gas and

379 rising the particles and the relative costs between heat and electrical power
 380 should be known.

381 5. Nomenclature

- 382 a_s Superficial area of the particle per unit of volume [m^{-1}]
 383 B Width of the MBHE in the direction perpendicular to both gas and
 384 solids flows [m]
 385 Bi Biot number [–]
 386 c Specific heat [$J/(kg K)$]
 387 c_p Specific heat at constant pressure [$J/(kg K)$]
 388 d_p Particle size [m]
 389 H Height of the MBHE in the direction of the particle flow [m]
 390 h_s Heat transfer coefficient [$W/(m^2 K)$]
 391 K Non-dimensional conductivity [–]
 392 k Conductivity [$W/(m K)$]
 393 L Length of the MBHE in the direction of the gas flow [m]
 394 \dot{m} Mass flow [kg/s]
 395 $MBHE$ Moving Bed Heat Exchanger
 396 P Gas pressure [Pa]
 397 \dot{Q} Heat transferred in the MBHE [W]
 398 t Time [s]
 399 T Gas temperature [K]

400	\hat{T}	Non-dimensional gas temperature [-]
401	\bar{T}	Mean gas temperature [K]
402	u	Velocity [m/s]
403	x	Horizontal coordinate (in the direction of the gas flow) [m]
404	y	Vertical coordinate (in the direction of the solids flow) [m]
405	\dot{W}_g	Power to pump the gas [W]
406	\dot{W}_s	Power to raise the particles [W]
407	<i>5.1. Greek symbols</i>	
408	γ	Ratio of the gas specific heats [-]
409	ΔP	Gas pressure drop through the MBHE [Pa]
410	ϵ_{MBHE}	Efficiency of the MBHE [-]
411	ϵ	Voidage of the MBHE [-]
412	η	Non-dimensional vertical coordinate [-]
413	θ	Solid temperature [K]
414	$\hat{\theta}$	Non-dimensional solid temperature [-]
415	$\bar{\theta}$	Mean solid temperature [K]
416	μ_g	Dynamic viscosity of the gas [Pa · s]
417	ξ	Non-dimensional horizontal coordinate [-]
418	ρ	Density [kg/m ³]

419 *5.2. Subscripts*420 g Gas phase421 in Inlet section422 out Outlet section423 s Solid phase424 w At the wall425 η η direction426 ξ ξ direction427 **References**

- 428 [1] S.S. Hsiau, J. Smid , F.H. Tsai, J.T. Kuo, C.S. Chou, Placement of
429 flow-corrective elements in a moving granular bed with louvered-walls,
430 Chemical Engineering and Processing, 43 (2004) 1037-1045.
- 431 [2] S.S. Hsiau, J. Smid, F.H. Tsai, J.T. Kuo, C.S. Chou, Velocities in moving
432 granular bed filters, Powder Technology, 114 (2001) 205-212.
- 433 [3] S.S. Hsiau, J. Smid , F.H. Tsai, J.T. Kuo, C.S. Chou, Velocity profiles of
434 granules in moving bed filters, Chemical Engineering Science, 54 (1999)
435 293-301.
- 436 [4] M. Socorro, A. Macias-Machin, J.M. Verona, D. Santana, Hot gas fil-
437 tration and heat exchange in a packed bed using Lapilli as a granular
438 medium, Industrial & Engineering Chemistry Research, 45 (2006) 7957-
439 7966.
- 440 [5] S. Yagi, D. Kunii, Studies on Heat Transfer Near Wall Surface in Packed
441 Beds, AIChE Journal, 6 (1960) 97-104.
- 442 [6] S. Yagi, D. Kunii, N. Wakao, Studies on axial effective thermal conduc-
443 tivities in packed beds, AIChE Journal 6 (1960) 543-546.

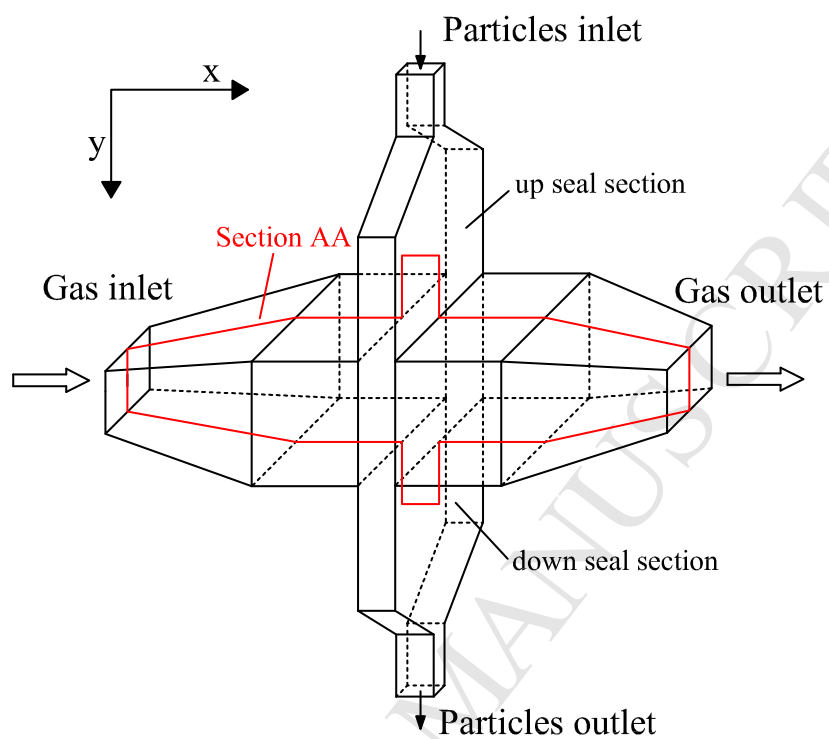
- 444 [7] A. Macías-Machín, A. Estevez, J. Cuellar, E. Jaraiz, Simple design of
445 crossflow moving-bed heat exchanger-filter (MHEF), *Filtration & Sepa-*
446 *ration*, 29 (1991) 155-161.
- 447 [8] E. Achenbach, Heat and flow characteristics of packed beds, *Experimen-*
448 *tal Thermal and Fluid Science*, 10 (1995) 17-27.
- 449 [9] A. Henriquez, A. Macias-Machin, Hot gas filtration using a moving bed
450 heat exchanger-filter (MHEF), *Chemical Engineering and Processing*,
451 36 (1997) 353-361.
- 452 [10] J.J. Saastamoinen, Heat exchange between two coupled moving beds by
453 fluid flow, *International Journal of Heat and Mass Transfer*, 47 (2004)
454 1535-1547.
- 455 [11] J.J. Saastamoinen, Comparison of moving bed dryers of solids operating
456 in parallel and counterflow modes, *Drying Technology*, 23 (2005) 1003-
457 1025.
- 458 [12] J. Smid, S.S. Hsiau, C.Y. Peng, H.T. Lee, Moving bed filters for hot gas
459 cleanup, *Filtration & Separation*, 42 (2005) 34-37.
- 460 [13] Y.S. Chen, S.S. Hsiau, S.C. Lai, Y.P. Chyoub, H.Y. Li, C.J. Hsua, Fil-
461 tration of dust particulates with a moving granular bed filter, *Journal*
462 *of hazardous materials*, 171 (2009) 987-994.
- 463 [14] J. Smid, S.S. Hsiau, C.Y. Peng, H.T. Lee, Granular moving bed fil-
464 ters and adsorbers (GM-BF/A) - patent review: 1970-2000, *Advanced*
465 *Powder Technology*, 16 (2005) 301-345.
- 466 [15] A. Niksiar, A. Rahimi, Design of a moving bed reactor for the production
467 of uranium tetrafluoride based on mathematical modeling, *Chemical*
468 *Engineering Science*, 65 (2010) 3147-3157.
- 469 [16] Z. Hongjun, S. Mingliang, W. Huixin, L. Zeji, J. Hongbo, Modeling and
470 Simulation of Moving Bed Reactor for Catalytic Naphtha Reforming,
471 *Petroleum science and technology*, 28 (2010) 667-676.
- 472 [17] K. Reijnen, J. van Brakel, Gas Cleaning at high temperatures and high
473 pressures: A review, *Powder Technology*, 40 (1984) 81-111.

- 474 [18] A. Macías-Machín, M. Socorro, J.M. Verona, M. Macías, New granular
475 material for hot gas filtration: Use of the Lapilli, *Chemical Engineering*
476 *and Processing*, 45 (2006) 719-727.
- 477 [19] A. Soria-Verdugo, J.A. Almendros-Ibáñez, U. Ruiz-Rivas, D. Santana,
478 Exergy optimization in a steady moving bed heat exchanger, *Annals of*
479 *the New York Academy of Sciences*, 1161 (2009) 584-600.
- 480 [20] G.D.R., Midi, On dense granular flows, *European Physical Journal E*,
481 14 (2004) 341-365.
- 482 [21] R.M. Nedderman, C. Laohakul, Thickness of the shear zone of flowing
483 granular-materials, *Powder Technology*, 25 (1980) 91-100.
- 484 [22] R.P. Zou, A.B. Yu, The packing of spheres in a cylindrical container -
485 the thickness effect, *Chemical Engineering Science*, 50 (1995), 1504-1507.
- 486 [23] H. Takahashi, H. Yanai, Flow profile and void fraction of granular solids
487 in a moving bed, *Powder Technology*, 7 (1973) 205-214.
- 488 [24] W. van Antwerpen, C.G. du Toit, P.G. Rousseau, A review of correla-
489 tions to model the packing structure and effective thermal conductivity
490 in packed beds of mono-sized spherical particles, *Nuclear Engineering*
491 *and Design*, 240 (2010) 1803-1818.
- 492 [25] M. Giese, K. Rottschäfer D. Vortmeyer, Measured and modeled super-
493 ficial flow profiles in packed beds with liquid flow, *AIChE Journal*, 44
494 (1998) 484-490.
- 495 [26] D. Vortmeyer, R.P. Winter, On the validity limits of packed-bed reac-
496 tor continuum models with respect to tube to particle diameter ratio,
497 *Chemical Engineering Science*, 39 (1984) 1430-1432.
- 498 [27] Y.S. Teplitskii, V.I. Kovenskii, M.V. Vinogradova, Phenomenological
499 model of heat transfer in an infiltrated granular bed at moderate
500 Reynolds numbers, *International Journal of Heat and Mass Transfer*,
501 80 (2007) 21-22.
- 502 [28] Y.H. Chen, X.D. Zhu, Y.Q. Wu, Z. Zhu, Investigation of the effect of
503 a dividing wall in a moving bed, *Chemical Engineering and Technology*,
504 30 (2007) 1028-1035.

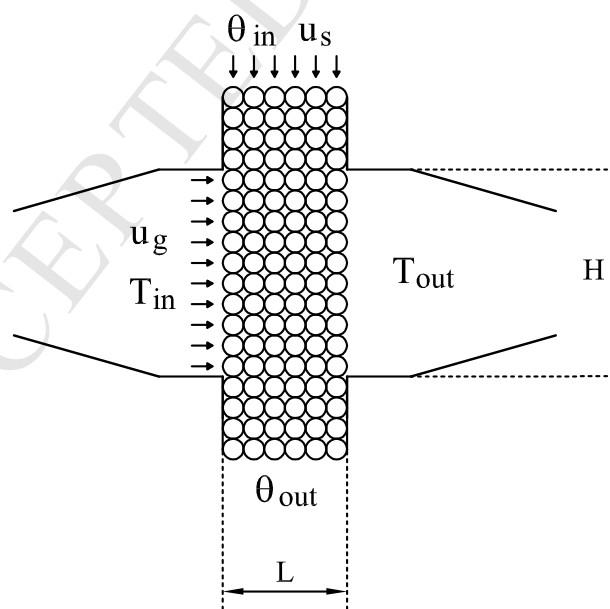
- 505 [29] R. Krupiczka, Analysis of thermal conductivity in granular materials,
506 International Chemical Engineering, 7 (1967) 122-144.
- 507 [30] C.M. Marb, D. Vortmeyer, Multiple steady-states of a cross-flow moving
508 bed reactor: theory and experiment, Chemical Engineering Science, 43
509 (1988) 811-819.
- 510 [31] D. Vortmeyer, R.J. Schaefer, Equivalence of one-phase and 2-phase mod-
511 els for heat-transfer processes in packed-beds-one-dimensional theory,
512 Chemical Engineering Science, 29 (1974) 485-491.
- 513 [32] J.J. Saastamoinen, Heat exchange between two coupled fixed beds by
514 fluid flow, International Journal of Heat and Mass Transfer, 46 (2003)
515 2727-2735.
- 516 [33] G. Nellis, S. Klein, Heat Transfer, Cambridge University Press, New
517 York, 2009.
- 518 [34] S. Ergun, Fluid flow through packed columns, Chemical Engineering
519 Progress, 48 (1952) 89-94.

520 **List of Figures**

521	1	Schematic of a Moving Bed Heat Exchanger (MBHE).	21
522	2	Nondimensional gas temperature profiles for the nominal MBHE.	
523		(a) analytical solution for $k_s = 0$, (b) numerical solution for	
524		$k_s = 1.5 W/(m K)$ and (c) numerical solution for the nominal	
525		case ($k_s = 15 W/(m K)$).	22
526	3	(a) Non-dimensional mean outlet gas temperature for different	
527		solid conductivities ($k_s = 0 - 0.75 - 1.5 - 8 - 15 W/(m K)$) and	
528		(b) $\xi_{x=L}$ for and optimum heat exchanger ($\xi_{x=L} = \eta_{y=H}$) with	
529		an efficiency of 90% ($\bar{T}_{out} = 0.1$) for different solid conductivities.	23
530	4	(a) Non-dimensional solid conductivity in the gas flow direc-	
531		tion K_ξ and (b) Biot number for the nominal data varying the	
532		particle size and the gas velocity. Figures (c) and (d) repre-	
533		sent respectively the non-dimensional conductivity K_ξ and the	
534		solid conductivity k_s in the limit case of $Bi = 0.1$	24
535	5	(a) Heat transferred retaining solid conductivity and (b) ne-	
536		glecting solid conductivity for different temperature differences.	
537		Figures (c) and (d) represent the power required to pump the	
538		gas and to raise the particles, respectively. The scale is in kJ/kg .	25



(a) General view



(b) View of section AA

Figure 1: Schematic of a Moving ²¹ Bed Heat Exchanger (MBHE).

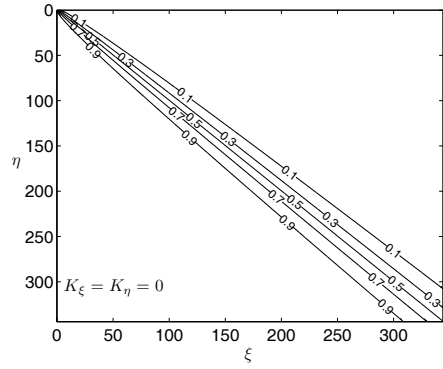
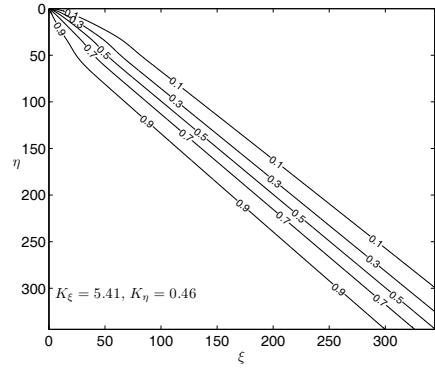
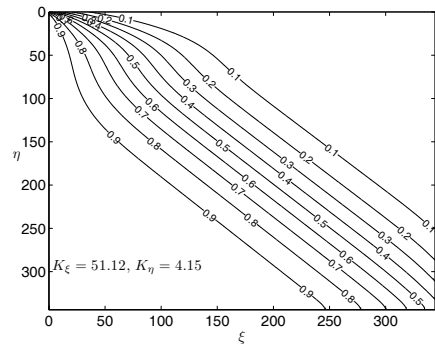
(a) $k_s = 0 W/(m K)$ (b) $k_s = 1.5 W/(m K)$ (c) $k_s = 15 W/(m K)$

Figure 2: Nondimensional gas temperature profiles for the nominal MBHE. (a) analytical solution for $k_s = 0$, (b) numerical solution for $k_s = 1.5 W/(m K)$ and (c) numerical solution for the nominal case ($k_s = 15 W/(m K)$).

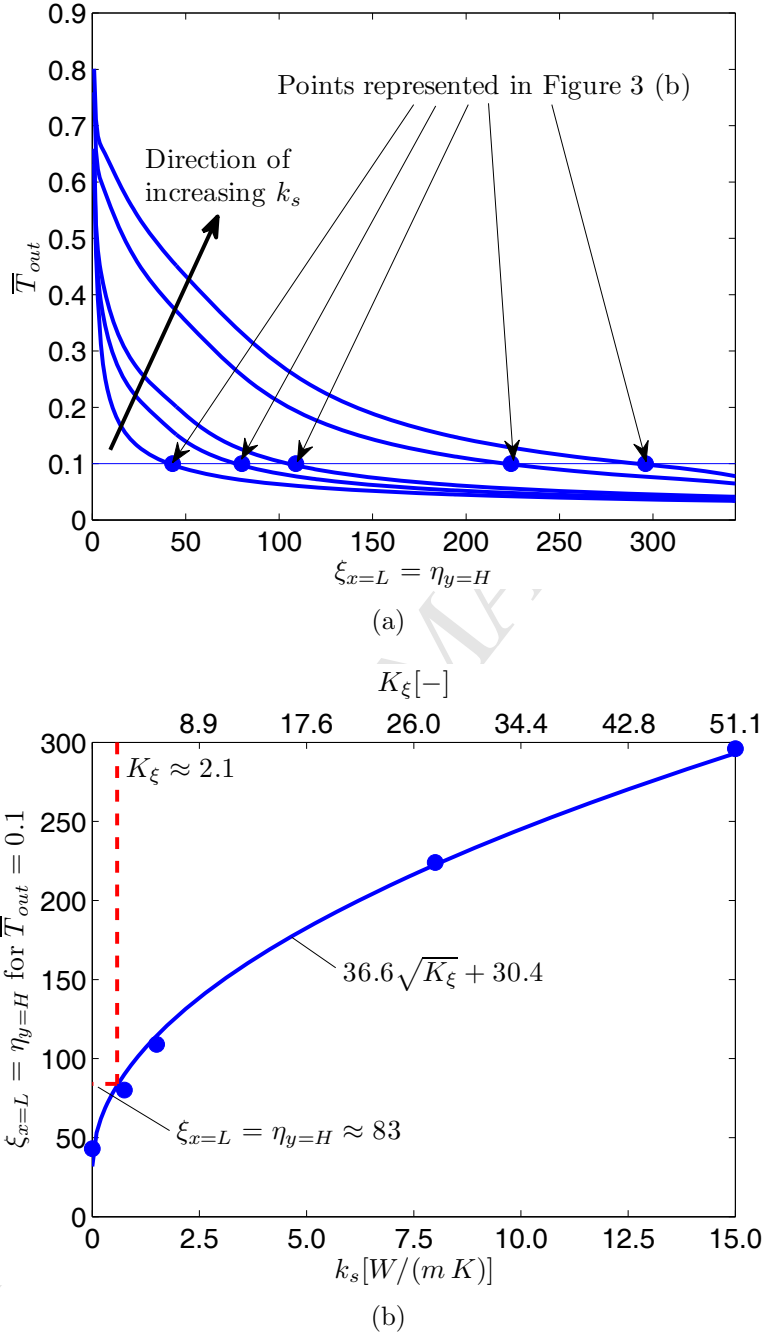


Figure 3: (a) Non-dimensional mean outlet gas temperature for different solid conductivities ($k_s = 0 - 0.75 - 1.5 - 8 - 15 W/(m K)$) and (b) $\xi_{x=L}$ for and optimum heat exchanger ($\xi_{x=L} = \eta_{y=H}$) with an efficiency of 90% ($\bar{T}_{out} = 0.1$) for different solid conductivities.

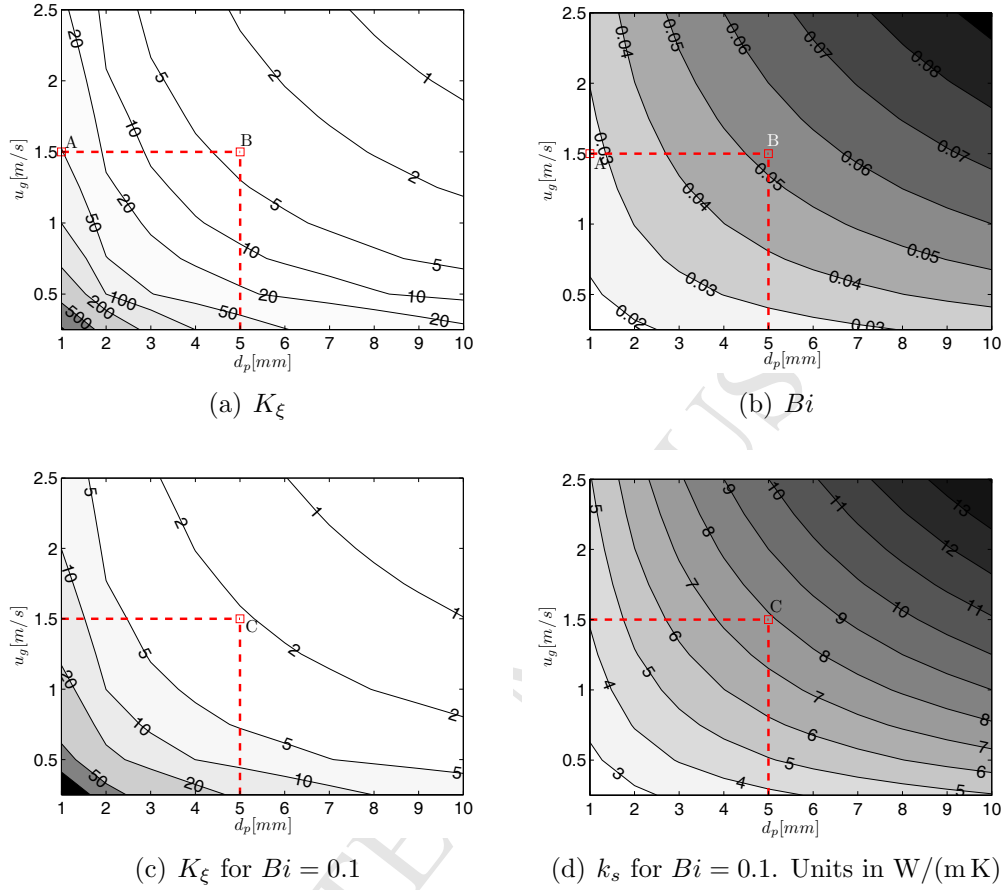


Figure 4: (a) Non-dimensional solid conductivity in the gas flow direction K_ξ and (b) Biot number for the nominal data varying the particle size and the gas velocity. Figures (c) and (d) represent respectively the non-dimensional conductivity K_ξ and the solid conductivity k_s in the limit case of $Bi = 0.1$.

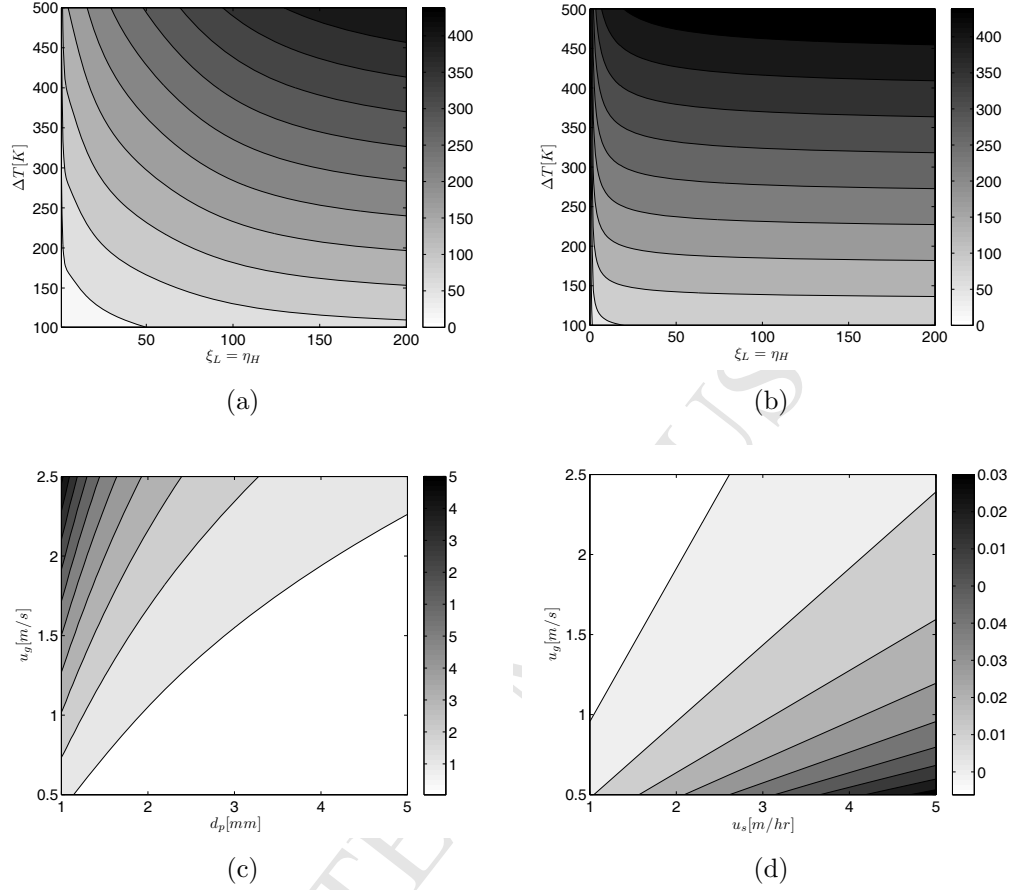


Figure 5: (a) Heat transferred retaining solid conductivity and (b) neglecting solid conductivity for different temperature differences. Figures (c) and (d) represent the power required to pump the gas and to raise the particles, respectively. The scale is in kJ/kg .

539 **List of Tables**

540	1	Experimental data of the work of Henriquez and Macías-Machín [9].	
541		Variables that are subject to variations throughout the paper	
542		are in bold format and capital letters.	27
543	2	Boundary conditions for solving equation system (3).	28
544	3	Non-dimensional parameters obtained with the nominal data	
545		of Henriquez and Macias-Machin [9].	29

GAS INLET TEMPERATURE T_{in}	100°C
Solid inlet temperature θ_{in}	25°C
GAS VELOCITY u_g	1.5 m/s
SOLID VELOCITY u_s	5 cm/min
Specific heat of the gas $c_{p,g}$	1005 J/(kg K)
Specific heat of the solids c_s	544 J/(kg K)
Gas density ρ_g	1 kg/m ³
Solid density ρ_s	7800 kg/m ³
Gas conductivity k_g	0.03 W/(m K)
SOLID CONDUCTIVITY k_s	15 W/(m K)
Gas dynamic viscosity μ_g	2.12×10^{-5} Pa · s
PARTICLE DIAMETER d_p	10^{-3} m
LENGTH IN THE DIRECTION OF THE GAS FLOW L	0.15 m
HEIGHT IN THE DIRECTION OF THE SOLIDS FLOW H	0.5 m
Bed porosity ε	0.4
Ratio of gas specific heats γ	1.4
Wall porosity ε_w	0.5
Gas pressure at the inlet section P_{in}	10^5 Pa

Table 1: Experimental data of the work of Henriquez and Macías-Machín [9]. Variables that are subject to variations throughout the paper are in bold format and capital letters.

Particles	$\xi = 0$	$\frac{\partial^2 \hat{\theta}}{\partial \xi^2} = 0$
	$\xi = \xi_L$	$\frac{\partial^2 \hat{\theta}}{\partial \xi^2} = 0$
	$\eta = 0$	$\hat{\theta} = K_\eta \frac{\partial \hat{\theta}}{\partial \eta}$
	$\eta = \eta_H$	$\frac{\partial \hat{\theta}}{\partial \eta} = 0$
Gas	$\xi = 0$	$\hat{T} = 1$

Table 2: Boundary conditions for solving equation system (3).

T_{in}	θ_{in}	$\xi_{x=L}$	$\eta_{y=H}$	K_ξ	K_η
1	0	363	344	51.12	4.15

Table 3: Non-dimensional parameters obtained with the nominal data of Henriquez and Macias-Machin [9].